Robustness of raw quantum tomography

M. Asorey [a], P. Facchi [b,c,d], G. Florio [e,c,d], V.I. Man'ko [f,*], G. Marmo [g,h,d], S. Pascazio [e,c,d], E.C.G. Sudarshan [i]

[a] *Departamento de Física Teórica, Facultad de Ciencias, Universidad de Zaragoza, 50009 Zaragoza, Spain*
[b] *Dipartimento di Matematica, Università di Bari, I-70125 Bari, Italy*
[c] *INFN, Sezione di Bari, I-70126 Bari, Italy*
[d] *MECENAS, Università Federico II di Napoli & Università di Bari, Italy*
[e] *Dipartimento di Fisica, Università di Bari, I-70126 Bari, Italy*
[f] *P.N. Lebedev Physical Institute, Leninskii Prospect 53, Moscow 119991, Russia*
[g] *Dipartimento di Scienze Fisiche, Università di Napoli "Federico II", I-80126 Napoli, Italy*
[h] *INFN, Sezione di Napoli, I-80126 Napoli, Italy*
[i] *Department of Physics, University of Texas, Austin, TX 78712, USA*

A B S T R A C T

We scrutinize the effects of non-ideal data acquisition on the tomograms of quantum states. The presence of a weight function, schematizing the effects of a finite window or equivalently noise, only affects the state reconstruction procedure by a normalization constant. The results are extended to a discrete mesh and show that quantum tomography is robust under incomplete and approximate knowledge of tomograms.

© 2010 Elsevier B.V. All rights reserved.

1. Introduction

Quantum technological applications require extremely accurate knowledge of quantum states and of the underlying quantum dynamical processes. For the application of fundamental principles of quantum mechanics and quantum optics to effectively foster the real-life implementation of quantum technologies, accurate quantum state characterization is a crucial ingredient at the interface between theoretical and experimental physics. Applications cover wide research areas ranging from nano-science to cosmology.

One of the most successful quantum state reconstruction techniques is quantum tomography [1,2] with its elegant experimental realizations [3–9]. For recent reviews, see [10,11]. A large class of quantum states, expressed in terms of Wigner functions, can be efficiently reconstructed by this method, including coherent states, Schrödinger cats, kittles, and entangled states. In quantum optics, the state can be directly measured by homodyne photon detection [12], providing as output result the optical tomogram. However, the precise characterization of quantum states becomes problematic, both for direct measurements and reconstruction procedures, when noise, imperfections and other practical problems deteriorate the quality or limit the size of the data set. This entails, from

an experimental perspective, a precise control/manipulation of the quantum system, from the source to the careful optimization of the detection apparatus, and from a theoretical perspective, the refinement of mathematical inversion techniques for noisy data and the extension of classical tomographic techniques to quantum situations [1,2,12–16].

In quantum applications, the most used tomographic methods are quantum generalizations of the Radon transform [17–19]. This is true both for massive particles and reconstruction methods based on homodyne photon detection. The measure of optical tomograms yields complete information on quantum states in terms of tomographic probability distributions [20]. Since, traditionally, one is interested in other equivalent characteristics of quantum states, like the Wigner or the Husimi or the diagonal coherent state representation function, we shall address here the question of the relation between these quantum state characteristics and our approach.

In practice the parameters introduced in the tomogram have many sources of uncertainty and an efficient tomographic measurement of the quantum state must face three major problems: (i) a finite window (including the effects of detectors, entailing coarse graining and/or binning of the data), (ii) the presence of random errors (arising both from the sample and the non-ideal precision in controlling the quadratures), and (iii) a discretized "mesh" in the data acquisition, that affects the generation of the quadratures of the tomogram.

---

* Corresponding author.
E-mail address: manko@lebedev.ru (V.I. Man'ko).

A realistic approach must define quantum tomograms through a convolution with a smooth weight function $\varXi$ that spreads the marginals and reduces to the usual "classical" Radon transform when $\varXi$ becomes a delta function. In this case one gets a kind of "thick tomography", in analogy with signal analysis, where a similar problem arises for signal detection and also requires the use of a window function [21,22]. Notice that in a classical description, where tomograms are measured by the attenuation of a probing beam scanning a material body, this would correspond to a finite transversal thickness of the scanning beam. However, this is only an analogy: in the physical situation we are describing there is no material body, nor probing beams, and the thickness is in phase space.

Our aim is to suggest extensions of the quantum tomographic techniques by taking into account the finiteness of the windows, the discreteness of data acquisition and the effects of noise, analogously to signal analysis. Previous work [23,24] focused on the definition of optimization strategies given a set of experimental data and non-ideal photodetector efficiency in homodyne detection (see also [25] for a review).

This Letter is organized as follows. In Section 2 we recall the main concepts related to the Radon and symplectic transforms. Section 3 is devoted to the effects of the finite window function. In Sections 4 and 5 we analyze how the tomograms are modified by noise and a discrete mesh. In Section 6 we present some numerical results for a particular example, corroborating our analysis. Finally, in Section 7 we sketch some conclusions and outline possible future research directions.

2. Preliminaries: Radon and symplectic transforms

We shall start by studying the role of the deformation associated with the window weight function in the experimental tomogram and its influence on the state reconstruction formula. The following framework is of general validity, and can be applied to massive particles as well as photons. However, for simplicity, let $\hat{\rho}$ be a given quantum photon state, $\hat{q}$ and $\hat{p}$ the position and momentum operators, and φ and X the local oscillator phase and quadrature in a homodyne experimental setup. The homodyne tomogram is given by

$$\mathcal{W}(X, \varphi) = \text{Tr}\{\hat{\rho}\delta(X - \hat{q}\cos\varphi - \hat{p}\sin\varphi)\}, \tag{1}$$

where $\text{Tr}\{A\}$ denotes the trace of the operator A. Expressed in terms of the Wigner function

$$W(p, q) = \frac{1}{\pi}\int_{\mathbb{R}}\langle q - \xi|\hat{\rho}|q + \xi\rangle e^{2ip\xi}\,d\xi, \tag{2}$$

the tomogram (1) reads

$$\mathcal{W}(X, \varphi) = \int_{\mathbb{R}^2} dp\,dq\,W(p, q)\delta(X - q\cos\varphi - p\sin\varphi). \tag{3}$$

The Radon transform of the Wigner function (3) has been generalized to the following symplectic, or M^2, transform [13,26]

$$\mathcal{W}^{\sharp}(X, \mu, \nu) = \int_{\mathbb{R}^2} W(p, q)\delta(X - q\mu - p\nu)\,dp\,dq, \tag{4}$$

with $\mu, \nu \in \mathbb{R}$. Its complete equivalence with (3) is expressed by the relation [27,28]

$$\mathcal{W}^{\sharp}(X, r\cos\varphi, r\sin\varphi) = \frac{1}{r}\mathcal{W}\left(\frac{X}{r}, \varphi\right), \tag{5}$$

valid for any $r > 0$. Eq. (5) is an easy consequence of the fact that the Dirac distribution is positive homogeneous of degree -1. The symplectic tomogram (4) can be easily inverted by a Fourier transform

$$W(p, q) = \int_{\mathbb{R}^3}\frac{dX\,d\mu\,d\nu}{(2\pi)^2}\mathcal{W}^{\sharp}(X, \mu, \nu)e^{i(X - q\mu - p\nu)}, \tag{6}$$

which by (5) yields the inversion formula

$$W(p, q) = \frac{1}{(2\pi)^2}\int_{\mathbb{R}} dX\int_{\mathbb{R}_+} dr\int_{\mathbb{T}} d\varphi\,\mathcal{W}(X, \varphi)$$
$$\times\,re^{ir(X - q\cos\varphi - p\sin\varphi)}, \tag{7}$$

where $\mathbb{T} = \mathbb{R}/2\pi\mathbb{Z}$ is the unit circle and $\mathbb{R}_+ = [0, +\infty)$.

3. Finite window

A finite window function can be accounted for by replacing the Dirac delta function in the definition of the tomogram (4) with a suitable smearing window function $\varXi$

$$\mathcal{W}^{\sharp}_{\varXi}(X, \mu, \nu) = \int_{\mathbb{R}^2} W(p, q)\varXi(X - q\mu - p\nu)\,dp\,dq. \tag{8}$$

Now, by Fourier transforming Eq. (8), one gets

$$W(p, q) = \mathcal{N}_{\varXi}\int_{\mathbb{R}^3}\frac{dX\,d\mu\,d\nu}{(2\pi)^2}\mathcal{W}^{\sharp}_{\varXi}(X, \mu, \nu)e^{i(X - q\mu - p\nu)}, \tag{9}$$

where

$$\mathcal{N}_{\varXi} = \frac{1}{\tilde{\varXi}(-1)}, \quad \tilde{\varXi}(-1) = \int_{\mathbb{R}}\varXi(z)e^{iz}\,dz. \tag{10}$$

In operator terms the state reconstruction is achieved by

$$\hat{\rho} = \mathcal{N}_{\varXi}\int_{\mathbb{R}^3}\frac{dX\,d\mu\,d\nu}{(2\pi)^2}\mathcal{W}^{\sharp}_{\varXi}(X, \mu, \nu)e^{i(X - \hat{q}\mu - \hat{p}\nu)}. \tag{11}$$

This is one of our central results: the inverse reconstruction map is *independent* of the window function, the only relic of the latter being the normalization constant $\mathcal{N}_{\varXi}$, that can be fixed by the normalization of one single tomogram. Thus, no matter how involved is the shape of the window function, an exact reconstruction of the state can be always achieved by means of (9) or (11). This property is very interesting because in practical cases the experimental window function $\varXi$ is unknown, but the result tells us that the exact state reconstruction is possible without any precise information about $\varXi$. This result is also independent of the features of the initial state, that can even be nonstationary. Interestingly, this result can be *extended* to situations were noise is present. This will be done in the next section.

4. Noise

We start from the following important observation: the effects of a spread function in the tomogram (8) are *de facto* equivalent to the presence of noise, due to quantum efficiency and/or thermalization, in a homodyne tomogram (e.g., if the quadrature is determined with a finite precision). The origin of such noise is due to the fact that any counting homodyne statistics is just a sampling of probabilities. Namely, any statistical event can be only approximately sampled and in the course of repeated measurements, the outputs are always fluctuating. All this can be seen as a jitter in the detected statistics.

The equivalence between such a jitter and a finite window can be seen as follows: if there is some jitter $X + \xi$ on X, where ξ is a random variable with a finite variance, one obtains

$$\mathcal{W}^{(\xi)}(X, \mu, \nu) = \text{Tr}\big\{\hat{\rho}\delta(X + \xi - \hat{q}\mu - \hat{p}\nu)\big\}. \tag{12}$$

By setting

$$\mathbb{E}\big[\delta(X + \xi)\big] = \varXi(X), \tag{13}$$

where $\mathbb{E}$ denotes the expectation value over the random variable ξ, one gets

$$\mathbb{E}\big[\mathcal{W}^{(\xi)}(X, \mu, \nu)\big] = \mathcal{W}_{\varXi}^{\sharp}(X, \mu, \nu) \tag{14}$$

and the reconstruction can be done exactly as above.

The jitter provides extra noise and deforms the output of homodyne experiments by affecting the basic inequalities of quantum mechanics expressed in terms of tomograms. For this reason, it is of practical interest to take it into account when extracting information on the uncertainty relations from the measurements of tomograms. In practice this can be done, for example, by using the output of photon homodyne measurements [3,11], given as optical tomograms (1). The quadrature (co)variances are directly expressed in terms of simple integrals containing optical tomograms [20,29] and can be used to yield a noise limit contribution to the experimental accuracy of uncertainty relations in homodyne photon detection.

Let us look at a simple but significant example of experimental relevance. Consider the Wigner function of the first excited state of a harmonic oscillator (or a single photon state)

$$W(p, q) = \frac{2(p^2 + q^2) - 1}{\pi}e^{-(p^2 + q^2)}. \tag{15}$$

Its Radon transform reads

$$\mathcal{W}(X, \varphi) = \frac{2X^2}{\sqrt{\pi}}e^{-X^2}. \tag{16}$$

The introduction of a Gaussian window function

$$\varXi(X) = \frac{1}{\sqrt{2\pi\sigma^2}}e^{-X^2/2\sigma^2}, \tag{17}$$

yields the symplectic tomograms

$$\mathcal{W}_{\varXi}^{\sharp}(X, \mu, \nu) = \frac{2(X^2/r^2 + \sigma^2(2\sigma^2 + 1))}{\sqrt{\pi}r(2\sigma^2 + 1)^{5/2}}e^{-X^2/r^2(2\sigma^2 + 1)}, \tag{18}$$

with $r = \sqrt{\mu^2 + \nu^2}$. Note that

$$\mathcal{W}_{\varXi}^{\sharp}(0, \mu, \nu) = \frac{2\sigma^2}{\sqrt{\pi r^2(2\sigma^2 + 1)^3}}. \tag{19}$$

Therefore, the presence of a window function/noise provokes a reduction of "visibility" of the tomogram (that would vanish for $\sigma = 0$). However, a perfect state reconstruction is obtained by Eq. (9) or (11).

This proves that an *exact* reconstruction can be obtained even in the presence of noise, provided one has very (in the limit, infinitely) accurate control over the position of the quadrature. This extends the central result of the preceding section.

5. Discreteness of data acquisition

So far we have assumed that the window function can be finite (thick tomograms), but one has access to all possible tomograms in a continuous range of parameters. We have not discussed the robustness of tomography with respect to the discreteness of data

acquisition. Let us assume that the experimental tomograms are gathered only on a sequence of discrete values of X and φ, namely

$$\mathcal{W}_{k,m} = \mathcal{W}\left(kT, m\frac{2\pi}{N}\right), \quad k \in \mathbb{Z}, \ m \in \mathbb{Z}_N \tag{20}$$

where $T > 0$, $\mathbb{Z}_N = \mathbb{Z}/N\mathbb{Z}$ and, for convenience, N is an odd positive integer. If the tomograms have a limited bandwidth, then for sufficiently small values of T and N^{-1} one can exactly reconstruct the whole family of tomograms from the knowledge of the experimental ones. This is the content of the Nyquist–Shannon sampling theorem [30,31]. More precisely, consider the Fourier transform of $\mathcal{W}$

$$\tilde{\mathcal{W}}(\omega, \ell) = \int_{\mathbb{R}} dX e^{-i\omega X} \int_{\mathbb{T}} \frac{d\varphi}{2\pi} e^{-i\ell\varphi}\mathcal{W}(X, \varphi). \tag{21}$$

If its support is compact and satisfies

$$\text{supp}\,\tilde{\mathcal{W}} \subset D, \quad D = \left(-\frac{\pi}{T}, \frac{\pi}{T}\right) \times \left(-\frac{N}{2}, \frac{N}{2}\right), \tag{22}$$

one has

$$\tilde{\mathcal{W}}(\omega, \ell) = \frac{T}{N} \sum_{k \in \mathbb{Z}} \sum_{m \in \mathbb{Z}_N} \mathcal{W}_{k,m} e^{-iX_k\omega}e^{-i\varphi_m\ell}\chi_D(\omega, \ell), \tag{23}$$

where $X_k = kT$, $\varphi_m = 2\pi m/N$, and

$$\chi_D(\omega, \ell) = \begin{cases} 1 & \text{if } (\omega, l) \in D, \\ 0 & \text{if } (\omega, l) \notin D. \end{cases} \tag{24}$$

Let us briefly show how (23) is obtained, by considering the less common situation of a function on the torus $\mathbb{T}$:

$$\tilde{f}(\ell) = \int_{\mathbb{T}} \frac{d\varphi}{2\pi} e^{-i\ell\varphi}f(\varphi), \quad f(\varphi) = \sum_{\ell \in \mathbb{Z}} e^{i\ell\varphi}\tilde{f}(\ell). \tag{25}$$

Suppose $\tilde{f}(\ell) = 0$ for $\ell \notin J$, with $J = (-N/2, N/2) \cap \mathbb{N}$. For definiteness let us assume N odd. Then $J = \{-(N-1)/2, \ldots, (N-1)/2\}$, and one can consider the periodic extension of $\tilde{f}$

$$\tilde{f}_N(\ell) = \sum_{k \in \mathbb{Z}} \tilde{f}(\ell - kN), \tag{26}$$

whose restriction to J coincides with $\tilde{f}$, namely,

$$\tilde{f}(\ell) = \tilde{f}_N(\ell)\chi_J(\ell). \tag{27}$$

This property would not be true if $\tilde{f}$ did not vanish outside J, and the phenomenon called aliasing would occur. One gets

$$\tilde{f}_N(\ell) = \int_{\mathbb{T}} \frac{d\varphi}{2\pi} e^{-i\ell\varphi} f(\varphi) \sum_{k \in \mathbb{Z}} e^{ikN\varphi}. \tag{28}$$

By recalling Poisson's formula

$$\sum_{k \in \mathbb{Z}} e^{ikN\varphi} = \frac{2\pi}{N} \sum_{k \in \mathbb{Z}} \delta(\varphi - \varphi_k), \tag{29}$$

with $\varphi_k = 2k\pi/N$, and setting $k = jN + m$ with $k, j \in \mathbb{Z}$ and $m \in \mathbb{Z}_N$ one gets

$$\sum_{k \in \mathbb{Z}} e^{ikN\varphi} = \frac{2\pi}{N} \sum_{m \in \mathbb{Z}_N} \sum_{j \in \mathbb{Z}} \delta(\varphi - \varphi_m - 2j\pi). \tag{30}$$

Therefore,

$$\tilde{f}_N(\ell) = \frac{1}{N} \sum_{m \in \mathbb{Z}_N} e^{-i\ell\varphi_m} f(\varphi_m). \tag{31}$$

By plugging (31) into (27) one gets the angular dependence of (23). The linear dependence is obtained analogously by replacing $\mathbb{T}$ with $\mathbb{R}$ and $\mathbb{Z}_N$ with $\mathbb{Z}$.

By Fourier inverting (27) one gets

$$
\begin{aligned}
f(\varphi) &= \sum_{\ell \in J} e^{i\ell\varphi} \tilde{f}_N(\ell) \\
&= \sum_{m \in \mathbb{Z}_N} f(\varphi_m) \frac{1}{N} \sum_{\ell \in J} e^{i\ell(\varphi - \varphi_m)} \\
&= \sum_{m \in \mathbb{Z}_N} f(\varphi_m) S_N\left(\frac{\varphi - \varphi_m}{2}\right),
\end{aligned}
\tag{32}
$$

with

$$
S_N(x) = \frac{\sin(Nx)}{N \sin x},
\tag{33}
$$

which is the extension of the sampling theorem to functions on the torus $\mathbb{T}$ and their discrete spectra. For a function $g(X)$ on the line, the analogous, well-know formula reads

$$
g(X) = \sum_{k \in \mathbb{Z}} g(X_k) \operatorname{sinc}\left(\pi \frac{X - X_k}{T}\right),
\tag{34}
$$

with $X_k = kT$ and $\operatorname{sinc} x = x^{-1} \sin x$.

Therefore, the tomograms are given, for N odd, by the (generalized) Shannon–Whittaker interpolation formula

$$
\begin{aligned}
\mathcal{W}(X, \varphi) &= \sum_{k \in \mathbb{Z}} \sum_{m \in \mathbb{Z}_N} \mathcal{W}_{k,m} \operatorname{sinc}\left(\pi \frac{X - X_k}{T}\right) \\
&\quad \times S_N\left(\frac{\varphi - \varphi_m}{2}\right), \quad \forall X \in \mathbb{R}, \forall \varphi \in \mathbb{T}.
\end{aligned}
\tag{35}
$$

For N even the formula is the same, by replacing N by $N - 1$ (since in that case the angular sampling points are $N - 1$ instead of N). Remarkably, for sufficiently small T and N^{-1} the reconstruction of limited-bandwidth tomograms is *faithful* and there is *no* information loss. It is interesting to observe that the application of signal-analysis techniques to quantum tomography can be quite straightforward. For example, from the mathematical point of view, the extension of Eqs. (32) and (35) of quantum tomograms to a torus is very natural.

By plugging (35) into (7) one can obtain a reconstruction formula of the Wigner function in terms of the tomographic samples (20). By writing

$$
\operatorname{sinc}\left(\pi \frac{X - X_k}{T}\right) = \frac{T}{2\pi} \int\limits_{-\pi/T}^{+\pi/T} e^{i\omega(X - X_k)} \, d\omega
\tag{36}
$$

and by performing the integration over X one gets a Dirac delta function $\delta(\omega + r)$ whose integral yields

$$
\begin{aligned}
W(p, q) &= \sum_{k \in \mathbb{Z}} \sum_{m \in \mathbb{Z}_N} \mathcal{W}_{k,m} \int\limits_{\mathbb{T}} d\varphi \, S_N\left(\frac{\varphi - \varphi_m}{2}\right) \\
&\quad \times \frac{T}{(2\pi)^2} \int\limits_{0}^{\pi/T} dr \, r e^{ir(X_k - q\cos\varphi - p\sin\varphi)}.
\end{aligned}
\tag{37}
$$

We get

$$
\begin{aligned}
\frac{T}{(2\pi)^2} \int\limits_{0}^{\pi/T} dr \, r e^{ir\beta} &= \frac{\alpha\sin\alpha + \cos\alpha - 1}{4T\alpha^2} \\
&\quad + i\frac{\alpha\cos\alpha - \sin\alpha}{4T\alpha^2},
\end{aligned}
\tag{38}
$$

with $\alpha = \pi\beta/T$. Since the imaginary part is odd with respect to the rotation $\varphi \to \varphi + \pi$, its integral over the torus vanishes and we finally obtain

$$
\begin{aligned}
W(p, q) &= \sum_{k \in \mathbb{Z}} \sum_{m \in \mathbb{Z}_N} \mathcal{W}_{k,m} \int\limits_{\mathbb{T}} d\varphi \, S_N\left(\frac{\varphi - \varphi_m}{2}\right) \\
&\quad \times \left[\frac{\cos(\alpha_k(\varphi; q, p)) - 1}{4T\alpha_k(\varphi; q, p)^2} \right. \\
&\quad \left. + \frac{\alpha_k(\varphi; q, p)\sin(\alpha_k(\varphi; q, p))}{4T\alpha_k(\varphi; q, p)^2}\right],
\end{aligned}
\tag{39}
$$

with $\alpha_k(\varphi; q, p) = \pi(X_k - q\cos\varphi - p\sin\varphi)/T$ (and N odd).

Let us now consider an experimental situation in which there is some uncertainty on the linear and angular position of the quadrature, that is

$$
\begin{aligned}
\mathcal{W}_{k,m}^{(\xi)} &= \mathcal{W}\left(X_k^{(\xi)}, \varphi_m^{(\xi)}\right), \\
X_k^{(\xi)} &= T\left(k + \xi_k^{(1)}\right), \qquad \varphi_m^{(\xi)} = \frac{2\pi}{N}\left(m + \xi_m^{(2)}\right),
\end{aligned}
\tag{40}
$$

with $k \in \mathbb{Z}$ and $m \in \mathbb{Z}_N$, where $\{\xi_k^{(1)}\}$ and $\{\xi_m^{(2)}\}$ are two sequences of independent identically distributed random variables with finite standard deviations $\sigma_\xi^{(1)}$ and $\sigma_\xi^{(2)}$. Under hypothesis (22), one gets

$$
\tilde{\mathcal{W}}(\omega, \ell) = \frac{T}{N} \mathbb{E}\left[\sum_{k \in \mathbb{Z}} \sum_{m \in \mathbb{Z}_N} \mathcal{W}_{k,m}^{(\xi)} e^{-iX_k^{(\xi)}\omega} e^{-i\varphi_m^{(\xi)}\ell} \chi_D(\omega, \ell)\right].
\tag{41}
$$

A Fourier transform, followed by a Radon inversion (11) yields on average a *perfect* reconstruction of the state. Therefore, quadrature uncertainties and unbiased noise do *not* affect the result.

Let us prove Eq. (41). Consider a function $g(X)$ on the line, with limited bandwidth, namely, $\tilde{g}(\omega) = 0$ for $\omega \notin I$, where $I = (-\pi/T, +\pi/T)$. One can write

$$
\begin{aligned}
h^{(\xi)}(\omega) &= \sum_{k \in \mathbb{Z}} g\left(X_k^{(\xi)}\right) e^{-iX_k^{(\xi)}\omega} \\
&= \sum_{k \in \mathbb{Z}} \int \frac{d\nu}{2\pi} \tilde{g}(\nu) e^{-iX_k^{(\xi)}(\omega - \nu)} \\
&= \int \frac{d\nu}{2\pi} \tilde{g}(\omega - \nu) \sum_{k \in \mathbb{Z}} e^{-iX_k^{(\xi)}\nu}.
\end{aligned}
\tag{42}
$$

By taking the expectation value, and by using Poisson's formula (29) one gets

$$
\begin{aligned}
\mathbb{E}\left[\sum_{k \in \mathbb{Z}} e^{-iX_k^{(\xi)}\nu}\right] &= \mathbb{E}\left[e^{-i\xi\nu}\right] \sum_{k \in \mathbb{Z}} e^{-iX_k\nu} \\
&= \frac{2\pi}{T} \mathbb{E}\left[e^{-i\xi\nu}\right] \sum_{k \in \mathbb{Z}} \delta\left(\nu - \frac{2\pi k}{T}\right).
\end{aligned}
\tag{43}
$$

Therefore,

$$
\mathbb{E}\left[h^{(\xi)}(\omega)\right] = \frac{1}{T} \sum_{k \in \mathbb{Z}} \tilde{g}\left(\omega - \frac{2\pi k}{T}\right) \mathbb{E}\left[e^{-i2\pi k\xi/T}\right],
\tag{44}
$$

that, when multiplied by $\chi_I(\omega)$, yields

$$
\mathbb{E}\left[h^{(\xi)}(\omega)\chi_I(\omega)\right] = \frac{1}{T} \tilde{g}(\omega)\mathbb{E}[1],
\tag{45}
$$

because of the condition on the bandwidth of g. Since $\mathbb{E}[1] = 1$, we get the linear dependence of (41), the proof of the angular dependence being analogous.

A comment seems in order. In our analysis we separately addressed the effects that arise from the existence of a finite window (or equivalently the presence of noise) and those that are a consequence of partial data acquisition. The problems that arise in non-ideal situations are under control in two limiting cases: when the window size σ and the sampling steps s $(= T, 1/N)$ are well separated, i.e. $\sigma \ll s$ or $s \ll \sigma$. The first case can be analyzed through Eq. (39), the second one through Eqs. (9)–(10). It would be interesting to understand whether a single general formula exists, that accounts at the same time for the consequences of all these effects and from which both above-mentioned cases arise as suitable limits. Such a formula would also enable us to elucidate whether the simple expression we obtained in terms of the normalization constant (10) can be generalized to the case of a finite number of measurements, or when noise is combined with other sources of uncertainty. This interesting aspect is left for future research. The following section is devoted to a partial numerical investigation of this problem.

6. Robustness of tomograms

So far, our analysis has taken into account the effects of noise and discreteness of data. We have seen that for sufficiently small T and N^{-1} the reconstruction of limited-bandwidth tomograms is faithful and there is no information loss [see Eq. (35) and following comments]. Also, quadrature uncertainties and unbiased noise do not affect the reconstruction [see Eq. (41) and following comments]. By combining all these results we now discuss the robustness of quantum tomograms under the afore-mentioned sources of uncertainty and limitations (discreteness of the sampling and finite precision in the determination of the quadrature, since we have already argued that a finite window is equivalent to the presence of noise). Let us look again at the tomogram (16) and numerically investigate the effects that arise due to a discrete mesh and the presence of noise on the Wigner function (15). We shall reconstruct the Wigner function by using Eq. (39) with $T = 0.1$, $N = 5$, and $\sum_{k \in \mathbb{Z}}$ replaced by $\sum_{|k| \leqslant K}$, with $K = 40$.

Fig. 1 shows the tomographic reconstructions of the Wigner function (15), starting from its tomograms (16). The Wigner function in the noiseless case is shown in the upper panel and is practically indistinguishable from the original (15). Notice that, even though the tomogram is not band limited and the number of points K is finite, the reconstruction by means of (39) is practically alias free. The reconstructions in the central and lower panel are affected by noise, as in (40) with zero means and $\sigma_\xi^{(1)} = \sigma_\xi^{(2)} = 0.5$: these are large values, of the same order of the sampling periods T and $2\pi/N$ (one should notice, however, that in this particular case the noise on the angular position of the quadrature does not affect the procedure due to the symmetry of the state considered). The central panel refers to a single realization of the noise, while the lower panel to an average over 10 realizations of the noise.

The reconstruction error is measured by the distance

$$
\begin{aligned}
\varepsilon &= \frac{1}{2} \| W - W_{\text{rec}} \|_B \\
&= \frac{1}{2} \int_B \left| W(p,q) - W_{\text{rec}}(p,q) \right| \, dp \, dq,
\end{aligned}
\tag{46}
$$

where B is the box considered (in our case $B = [-1.5, 1.5]^2$). We obtain $\varepsilon = 1.4 \times 10^{-4}, 0.11, 0.028$ for the upper, central and lower panel, respectively. This should be compared with $\|W\|_B = 1.01$. It is apparent both from Fig. 1 and the above numerical results that the reconstruction is robust *at the same time* against noise and discretization effects.
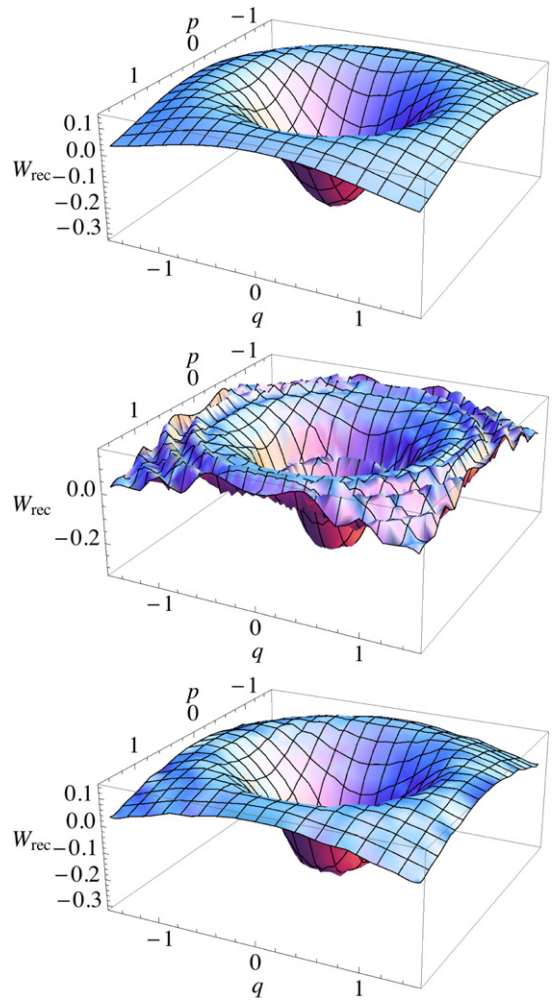

Fig. 1. Reconstruction starting from the tomograms (16) of the Wigner function $W(p,q)$ in Eq. (15). We set $N = 5$, $T = 0.1$ and $K = 40$ in Eqs. (39) and (41). Upper panel: no noise. The reconstructed and the original function are indistinguishable. Central panel: single noise realization, $\sigma_\xi^{(1)} = \sigma_\xi^{(2)} = 0.5$. Lower panel: average over 10 realizations of the noise.

7. Conclusions

In conclusion, we have discussed the practical problems that arise in quantum (homodyne) tomography. First of all, the presence of a weight function has been shown to introduce only a normalization constant, which entails no loss of information and permits the exact reconstruction without any precise knowledge of the window function of the experimental setup: on average, quadrature uncertainties and unbiased noise do not affect the reconstruction. Second, the discretization procedure affects the global reconstruction in the same way as it does in the classical Nyquist–Shannon setting: if the bandwidth of the tomogram is limited, there is no information loss for a sufficiently dense sampling. We have also discussed the most general case, in which both problems arise simultaneously. Although we were not able to derive a general formula, from which both sources of non-ideal data acquisitions are present at the same time, and from which both situations investigated here are derived as limiting cases, we proved by numerical methods the robustness of the overall reconstruction against the different sources of imperfections. The validity of the approach proposed here should be tested in conjunction with other refined theoretical tools based on the maximum likelihood estimation [14,15,23].

Since nowadays quantum states reconstruction is based on the measurement of tomograms, the robustness against non-ideal data

acquisition provides solid foundation to the compatibility of tomographic experiments performed in different laboratories by different methods. Our results provide therefore a solid basis for the theoretical and phenomenological analysis of real tomograms.

Acknowledgements

References

[1] J. Bertrand, P. Bertrand, Found. Phys. 17 (1987) 397.
[2] K. Vogel, H. Risken, Phys. Rev. A 40 (1989) 2847.
[3] D.T. Smithey, M. Beck, M.G. Raymer, A. Faridani, Phys. Rev. Lett. 70 (1993) 1244.
[4] C. Kurtsiefer, T. Pfau, J. Mlynek, Nature 386 (1997) 150.
[5] G. Badurek, et al., Phys. Rev. A 73 (2006) 032110.
[6] T. Kiesel, W. Vogel, V. Parigi, A. Zavatta, M. Bellini, Phys. Rev. A 78 (2008) 021804R.
[7] V. D'Auria, S. Fornaro, A. Porzio, S. Solimeno, S. Olivares, M.G.A. Paris, Phys. Rev. Lett. 102 (2009) 020502.
[8] A. Zavatta, V. Parigi, M.S. Kim, H. Jeong, M. Bellini, Phys. Rev. Lett. 103 (2009) 140406.
[9] A. Allevi, A. Andreoni, M. Bondani, G. Brida, M. Genovese, M. Gramegna, S. Olivares, M.G.A. Paris, P. Traina, G. Zambra, Phys. Rev. A 80 (2009) 022114.
[10] M.G.A. Paris, J. Řeháček (Eds.), Quantum State Estimation, Lecture Notes in Physics, vol. 649, Springer, Berlin, 2004.
[11] A.I. Lvovsky, M.G. Raymer, Rev. Mod. Phys. 81 (2009) 299.
[12] S. Mancini, V.I. Man'ko, P. Tombesi, Phys. Lett. A 213 (1996) 1.
[13] V.I. Man'ko, G. Marmo, A. Simoni, A. Stern, E.C.G. Sudarshan, Phys. Lett. A 35 (2005) 351.
[14] P. Banáš, J. Řeháček, Z. Hradil, Phys. Rev. A 74 (2006) 014101.
[15] Z. Hradil, D. Mogilevtsev, J. Řeháček, Phys. Rev. Lett. 96 (2006) 230401.
[16] Z. Hradil, J. Řeháček, Z. Bouchal, R. Celechovsky, L.L. Sanchez-Soto, Phys. Rev. Lett. 97 (2006) 243601.
[17] J. Radon, Math.-Phys. Klasse 69 (1917) 262.
[18] F. John, Plane Waves and Spherical Means: Applied to Partial Differential Equations, Wiley–Interscience, New York, 1955.
[19] R.S. Strichartz, Amer. Math. Monthly 89 (1982) 377.
[20] A. Ibort, V.I. Man'ko, G. Marmo, A. Simoni, F. Ventriglia, Phys. Scr. 79 (2009) 065013.
[21] L. Cohen, Proc. IEEE 77 (1989) 941.
[22] D. Gabor, J. IEEE (London) 93 (1946) 429.
[23] K. Banaszek, G.M. D'Ariano, M.G.A. Paris, M.F. Sacchi, Phys. Rev. A 61 (2000) 010304.
[24] L.M. Artiles, R.D. Gill, M.I. Guta, J. Royal Stat. Soc. Ser. B (Stat. Methodology) 67 (2005) 109.
[25] M. Hayashi (Ed.), Asymptotic Theory of Quantum Statistical Inference, World Scientific, Singapore, 2005.
[26] O.V. Man'ko, V.I. Man'ko, G. Marmo, Phys. Scr. 62 (2000) 446;
O.V. Man'ko, V.I. Man'ko, G. Marmo, J. Phys. A: Math. Gen. 35 (2002) 699.
[27] P. Facchi, M. Ligabò, S. Pascazio, J. Mod. Opt. 57 (2010) 239.
[28] P. Facchi, M. Ligabò, AIP Conf. Proc. 1260 (2010) 3.
[29] V.I. Man'ko, G. Marmo, A. Simoni, F. Ventriglia, Adv. Sci. Lett. 2 (2009) 517.
[30] H. Nyquist, Trans. AIEE 47 (1928) 617, Reprinted as classic paper in: Proc. IEEE 90 (2002) 180.
[31] C.E. Shannon, Proc. Inst. Radio Eng. 37 (1949) 10, reprinted as classic paper in: Proc. IEEE 86 (1998) 447.